

An algorithm for calving flux retrieval

Erling Johnson^{1,2}, Lina Han¹, Dana Floricioiu¹ and Michael Bässler¹

¹Remote Sensing Technology Institute, German Aerospace Center (DLR IMF), Oberpfaffenhofen, Germany

²Universidad de Magallanes, Punta Arenas, Chile

Introduction

Recent global low-resolution mass estimates from glaciers and ice caps show a significant deficit for many ice-covered regions over the world. The uncertainty on the mass balance is still very high, in particular for calving glaciers, which are the main contributors to ice loss in certain climatic sensitive areas. Therefore, the development of a method for the estimation of the net mass balance component due to the ice export (calving) is needed. The present work resumes the methodology to automatically estimate the calving rate and flux in a test area.

Dataset and Methods

Glacier velocity

The glacier velocity is calculated by an amplitude correlation algorithm applied to pairs of high resolution geocoded TerraSAR-X images with 11 days repeat pass.

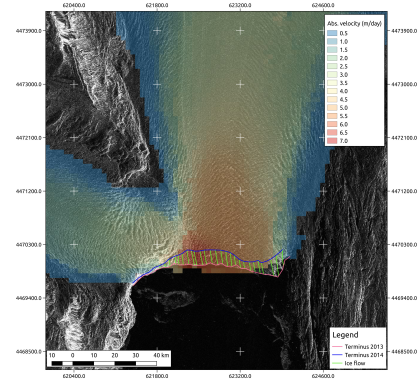


Figure 1 Absolute velocities from Upsala glacier (49° 53' 13''S, 73° 16' 21''W) calculated between 14.08.2013 and 25.08.2013. The automatically obtained frontal positions and the ice flow lines are shown.

Surface elevation

The glacier Digital Elevation Model (DEM) was generated from TanDEM-X bistatic data. The Integrated TanDEM-X Processor (ITP) (Rossi et al., 2012) at DLR was used to perform the full interferometric processing. Afterwards a correction of the absolute elevation in terms of absolute phase offset was performed.

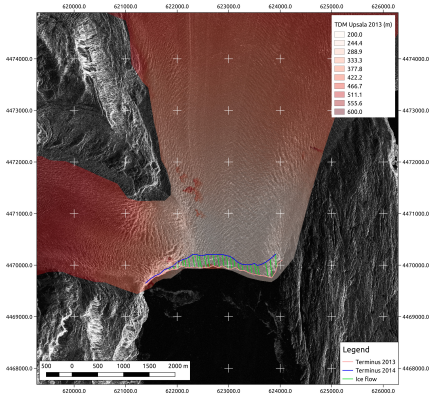


Figure 2 TanDEM-X surface elevation of Upsala glacier on 28.01.2013 with glacier terminus and ice flowlines.

References:
 Gebco gridded global bathymetry data (2009). *British Oceanographic Data Centre, Liverpool, United Kingdom.*
 Han, L. (2016). Development of an algorithm for the detection of calving glaciers frontal position from TerraSAR-X imagery. *master thesis DLR/IMF.*
 Rossi, C., Rodriguez Gonzalez, F., Fritz, T., Yague-Martinez, N., & Eineder, M. (2012). TanDEM-X calibrated Raw DEM generation. *ISPRS Journal of Photogrammetry and Remote Sensing*, 73, 12–20.
 Schaefer, M., Machguth, H., Falvey, M., Casassa, G., & Rignot, E. (2015). Quantifying mass balance processes on the Southern Patagonia Icefield. *The Cryosphere*, 9(1), 25–35.
 Skvarca, P., & De Angelis, H. (2001). Bathymetric survey in the vicinity of calving Glacier Upsala, Lago Argentino, southern Patagonia, Argentina. *Glaciological and Geomorphological Studies in Patagonia.*

Calving rate

The calving rate u_c , defined as the volume of ice that breaks off per unit of time and per unit of vertical area from glacier terminus, is determined as:

$$u_c = u_T - \Delta x / \Delta t$$

u_T - ice velocity at the glacier front.

$\Delta x / \Delta t$ - length change of terminus over time.

TerraSAR-X velocity at front is used to obtain u_T and a series of flow lines L_i . By means of automatically obtained glacier fronts (Han, 2016) and the flow lines Δx is calculated.

Calving flux

The calving flux Q_c represents the volume of ice that a glacier is losing on the terminus in a determined period of time. It can be estimated using an empirical relationship (Schaefer et al., 2015):

$$Q_h = \langle h \rangle \cdot \langle w \rangle \cdot u_c$$

$\langle h \rangle$ - mean frontal glacier width.

$\langle w \rangle$ - mean glacier thickness (difference between DEM and bathymetry).

The calving fluxes were calculated between two ice flowlines forming several flux gates "G_i" of width w_i along the front.

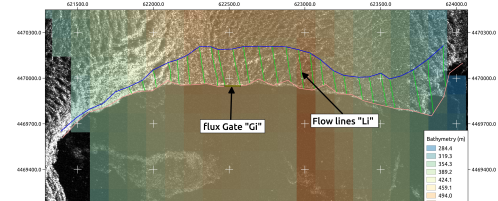


Figure 3 Interpolated bathymetry from General Bathymetric Charts (GEBCO) and data from Skvarca et al., 2001.

Results and conclusions

Table 1 Calving rate values for every glacier flow line "L_i"

L1 (m/d)	L2 (m/d)	L3 (m/d)	L4 (m/d)	L5 (m/d)	L6 (m/d)	L7 (m/d)	L8 (m/d)	L9 (m/d)
2.343	2.895	4.515	5.569	6.001	6.454	7.043	6.290	7.029
L10 (m/d)	L11 (m/d)	L12 (m/d)	L13 (m/d)	L14 (m/d)	L15 (m/d)	L16 (m/d)	L17 (m/d)	L18 (m/d)
6.857	6.559	6.524	6.405	6.331	6.387	6.151	5.915	5.875
L19 (m/d)	L20 (m/d)	L21 (m/d)	L22 (m/d)	L23 (m/d)	L24 (m/d)	L25 (m/d)	L26 (m/d)	
5.735	5.536	5.293	5.231	5.111	3.272	2.341	1.464	

Table 2 Calving fluxes on every gate "G_i"

G1 (km ³ /y)	G2 (km ³ /y)	G3 (km ³ /y)	G4 (km ³ /y)	G5 (km ³ /y)	G6 (km ³ /y)	G7 (km ³ /y)	G8 (km ³ /y)
0.018377	0.034449	0.031942	0.041880	0.058162	0.050225	0.032826	0.065193
G9 (km ³ /y)	G10 (km ³ /y)	G11 (km ³ /y)	G12 (km ³ /y)	G13 (km ³ /y)	G14 (km ³ /y)	G15 (km ³ /y)	G16 (km ³ /y)
0.036734	0.057629	0.059350	0.058451	0.070376	0.047512	0.030203	0.033775
G17 (km ³ /y)	G18 (km ³ /y)	G19 (km ³ /y)	G20 (km ³ /y)	G21 (km ³ /y)	G22 (km ³ /y)	G23 (km ³ /y)	TOTAL (km ³ /y)
0.042477	0.069845	0.040633	0.039705	0.039593	0.071402	0.044267	1.07501

- The calving rate values at the Upsala glacier are slightly higher than the terminus velocity, which indicates a loss of mass.
- The calving rate in 2013-2014 at Upsala glacier shows a reduced calving activity compared to the period 2000-2011 (Schaefer et al., 2015).
- The calving flux result can be improved using a denser flowline net in order to obtain the frontal area.

Acknowledgments:

This work was partially supported by the German Academic Exchange Service (DAAD) and Becas Chile (CONICYT).

